Regulated compartmentalization of enzymes in Golgi by GRASP55 controls cellular glycosphingolipid profile and function

Prathyush Pothukuchi[1], Ilenia Agliarulo[1#], Marinella Pirozzi[1#], Riccardo Rizzo[1], Domenico Russo[1], Gabriele Turacchio[1], Laura Capolupo[2], Maria Jose Hernandez-Corbacho[5], Giovanna Vanacore[1], Nina Dathan[1], Petra Henklein[3], Julian Nüchel[4], Markus Plomann[4], Lina M. Obeid[5], Yusuf A. Hannun[5], Alberto Luini[1], Giovanni D'Angelo[2], Seetharaman Parashuraman[1*]

[1] Institute of Biochemistry and Cell Biology, National Research Council of Italy, Via P. Castellino, 111, 80131, Italy.

[2] École Polytechnique Fédérale de Lausanne (EPFL), AI 1109 (Bâtiment AI), Station 19, CH-1015 Lausanne, Switzerland.

[3] Universitätsmedizin Berlin Institut für Biochemie Charité CrossOver Charitéplatz 1 / Sitz: Virchowweg 610117 Berlin, Germany.

[4]Center for Biochemistry, Joseph-Stelzmann-Strasse 52, D50931 Cologne, Germany.

[5] Stony Brook University Medical Center, Stony Brook 11794-8430, New York, United States.

# These authors contributed equally.

Running title: Golgi compartmentalization regulates glycosylation

* Correspondence to: SP - raman@ibbc.cnr.it

Abstract

Glycans are important regulators of cell and organismal physiology. This requires that the glycan biosynthesis be controlled to achieve specific cellular glycan profiles. Glycans are assembled in the Golgi apparatus on secretory cargoes that traverse it. The mechanisms by which Golgi apparatus ensures cell and cargo-specific glycosylation remain obscure. We investigated how Golgi apparatus regulates glycosylation by studying biosynthesis of glycosphingolipids, glycosylated lipids with critical roles in signalling and differentiation. Glycosylation enzymes have compartmentalized localization in the Golgi stack, but the molecular machineries involved are unknown. We identified Golgi matrix protein GRASP55 as a prototype controller of Golgi enzyme localization that specifically binds and compartmentalizes key glycosphingolipid biosynthetic enzymes by promoting their anterograde transport in the Golgi. Impairing GRASP55-enzyme interaction decompartmentalizes these enzymes, changes the cargo flux across competing glycosylation pathways that results in alteration of cellular glycosphingolipid profile. This GRASP55 regulated pathway of enzyme compartmentalization allows cells to make cell density dependent adaptations to glycosphingolipid biosynthesis to suit cell growth needs. Thus, Golgi apparatus controls cellular glycan (glycosphingolipid) profile by governing competition between biosynthetic reactions through regulated changes in enzyme compartmentalization.

Introduction

Glycans are one of the fundamental building blocks of the cell and play key roles in development and physiology (*1-5*). Cellular glycan profiles are sensitive to changes in cell state and/or differentiation and are also important contributors to the process (*6*). Indeed, several developmental disorders are associated with impaired production of glycans (*7*). Thus, how the glycan biosynthesis is regulated to achieve specific cellular glycan profiles is an important biological problem. In eukaryotes, glycans are assembled mainly by the Golgi apparatus on cargo proteins and lipids that traverse the organelle (*8*). Glycan biosynthesis happens in a template-independent fashion (*9*), yet the products are not random polymers of sugars but a defined distribution of glycans that is cell-type and cargo-specific (*9, 10*). This suggests that their biosynthesis is guided by regulated program(s). Indeed, transcriptional programs contribute to defining the glycome of a cell, but only partially (*9, 11, 12*). An obviously important but unexplored factor that influences glycosylation is the Golgi apparatus itself (*13, 14*).

The Golgi apparatus is a central organelle of the secretory pathway that processes newly synthesized cargoes coming from the endoplasmic reticulum (ER), primarily by glycosylation, before sorting them towards their correct destination in the cell. It consists of a stack of 4-11 cisternae (*15*), populated by enzymes and accessory proteins that maintain suitable milieu for the enzymes to act. The stack is polarized with a *cis*-side where cargoes arrive and a *trans*-side from where they leave. The enzymes are not homogenously distributed across the Golgi stack but are restricted or compartmentalized to 1-3 specific cisternae. The cisternal maturation model provides a conceptual framework for understanding Golgi enzyme compartmentalization (*16, 17*). According to the model, Golgi localization of enzymes in the face of anterograde flux of cargoes is mediated by their retrograde flux promoted by coat protein complex I (COPI) machinery (*18-22*) and assisted by Conserved oligomeric complex (COG) proteins and Golgi matrix proteins especially Golgins (*23-25*). However, the specific molecular mechanisms and processes by which the same retrograde transport pathway promotes localization of enzymes to distinct cisternae remain unknown.

This compartmentalized localization of enzymes is expected to play an important role in glycosylation since their localization along the *cis-trans* axis usually reflects their order of action (*26*). The sequential localization of enzymes in the Golgi is expected to be of considerable importance in case of competing reactions, which are prevalent in glycosylation pathways. When two or more enzymes compete for a substrate, the order in which they get access to it will substantially influence the products obtained and subsequently their functional outcomes. Thus, controlling the compartmentalized localization of competing reactions is of utmost importance to

ensure specific glycan output (*27, 28*). Nevertheless, how and to what extent compartmentalized enzyme localization in the Golgi is regulated to influence glycosylation reactions and its physiological relevance remains uncertain.

To evaluate and understand the contribution of Golgi compartmentalization in regulating glycosylation, we have focused our study on sphingolipid (SL) glycosylation. We chose this model system since the biosynthetic pathway is well characterized from both biochemical and transcriptional perspectives (*6, 29, 30*) and for the importance of SLs in physiology and development (*31, 32*). The SL glycosylation pathway exhibits the essential features of glycosylation pathways like localization of enzymes reflecting their order of action and also two well-characterized competing reactions steps that are important in determining the metabolic outcome of the pathway (see below). Further, while enzymes of the pathway are well characterized, molecular players regulating their sub-Golgi compartmentalization are unknown. Here, we identify GRASP55 as an important factor that specifically binds and compartmentalizes two key enzymes located at critical branching points of the SL glycosylation pathway. GRASP55 acts in an unexpected and novel way to promote the anterograde transport of enzymes to achieve the compartmentalization. This positions the competing enzymes at appropriate levels in the Golgi stack so as to regulate cargo flux across competing reactions of the pathway and determine the metabolic outcome *viz*. sphingolipid profile of the cell. Further, the alterations in the SL metabolic outcome due to GRASP55-dependent changes in enzyme compartmentalization control density dependent cell growth. These results delineate a molecular mechanism of enzyme compartmentalization and highlight the physiological importance of this mechanism in regulated production of cell surface glycans.

Results:

Disruption of Golgi organization alters SL biosynthesis:

SL biosynthesis starts with the production of ceramide (Cer) in the ER, which is then processed in the Golgi to sphingomyelin (SM) or glycosphingolipids (GSLs). The model cell system we use, HeLa cells, produces two species of GSLs - globosides (Gb3) and gangliosides (GM1 and GM3) (*6, 29, 30*) (See **Fig.1A** for schematic of the SL system in HeLa cells). This SL pathway includes sequential processing of Cer to complex GSLs as well as two bifurcating steps where the substrates get differentially channelled. The first is the bifurcation between SM and glucosylceramide (GlcCer) biosynthesis, where the substrate Cer is channelled into either of the pathways. The second is the biosynthesis of Gb3 or GM3 from lactosylceramide (LacCer). These two critical steps determine the amount and type of SLs produced by the cell. We

examined the localization of SL biosynthetic enzymes and found that they localize to three distinct zones in the secretory pathway **(Fig.1B,S1)**: (a) the early secretory pathway including the ER and the *cis/medial*-Golgi (C1, C2 cisternae), where Cer biosynthetic enzymes are localized (*33*), have little if any SL biosynthetic enzymes except for a slightly elevated amount of GM3S and GCS in the cis/medial-Golgi compared to other GSL biosynthetic enzymes; (b) *medial/trans*-Golgi (C3, C4 cisternae) where most of the GSL biosynthetic enzymes are present alongside substantial amounts of Sphingomyelin synthase 1 (SMS1) and (c) *trans*-Golgi network (TGN), where SMS1 predominates. While all the GSL biosynthetic enzymes show a gradient of increasing concentration from cis to *trans*- Golgi, the gradient is much sharper in the case of GB3S and LCS compared to GCS and GM3S **(Fig.S1)**. Thus, the SL biosynthetic enzymes are distributed reflecting their order of action with precursor (Cer) producing enzymes in the early secretory pathway and the Cer processing enzymes in late secretory pathway, which is in turn divided into two distinct zones where GSL and SM biosynthesis predominate. Of note, we expressed HA-tagged enzymes (see Methods) for our studies since the endogenous enzyme were barely detectable and/or efficient antibodies for EM studies were not available. We also note that the localization of GCS has been reported to be on the *cis*-side of the Golgi (*30*) contrary to what we report here. This is probably because the earlier studies had used a construct with a tag that blocks the signal for intra-Golgi localization (see below). Next, SL output of this system was measured by metabolic pulse-chase labelling with ^{3}H-sphingosine, a precursor of ceramide. This revealed the following distribution of products at steady state: SM (70%), globosides (10%) and gangliosides (5%) and rest remaining as precursors (Cer, GlcCer or LacCer; 15%) **(Fig.1C,D)**. The GSLs (globosides, gangliosides and GSL precursors GlcCer and LacCer) together constituted 25% of total SLs produced. We will refer to the ratio of GSL:SM::25:70 as SL output and the ratio of gangliosides (GM) to Globosides (Gb), GM:Gb::5:10 as GSL output **(Fig.1D)**. For simplicity the SL output will be represented as GSL levels since a change in GSL level is always associated with a proportional change in SM levels in the opposite direction. For GSL output, the situation is complex since a substantial portion of signal remains as precursors (GlcCer and LacCer) and so GSL output will be represented as a GM/Gb ratio which under the control conditions corresponds to 0.5 (GM:Gb::5:10). To summarize, SL machinery has a compartmentalized localization across the Golgi in HeLa cells and produces a SL output such that 70% of the Cer is directed towards the production of SM and 25% towards the production of GSLs. Within this 25%, 5% is directed towards the production of gangliosides and 10% towards the production of globosides.

This differential distribution of glycoforms produced by the Golgi apparatus has largely been ascribed to the differential expression of the corresponding glycosylation enzymes (*11-13*). To assess the contribution of enzyme compartmentalization to this, we monitored SL output after disrupting the spatial organization of SL biosynthetic enzymes by a) overexpressing GTP locked mutants of monomeric GTPases - secretion associated Ras related GTPase (Sar1 H79G) and ADP ribosylation factor 1 (ARF1 Q71L) that are well-known to disorganize the secretory pathway (*34, 35*) and b) by treating the cells with Brefeldin A, which causes relocation of Golgi enzymes back to ER. Overexpression of Sar1 H79G led to collapse of Golgi apparatus into ER with SL biosynthetic enzymes showing a reticular ER pattern **(Fig.S2A)**. On the other hand, overexpression of ARF1 Q71L mutant led to disruption of stacked cisternal structure of Golgi, which was replaced by tubulo-vesicular clusters **(Fig.S2B)**, with no separation between *cis* and *trans*-Golgi markers **(Fig.S2C)**. The treatment with Brefeldin A led to the translocation of the enzymes back into the ER as expected, apart from SMS1 which while mostly present in the ER also displayed presence in some spotty structures **(Fig.S2A)**. The SL output at steady state was altered in these cells, and consistently in all three conditions there was an increased production of GSLs over SM and gangliosides over globosides **(Fig.S2D,E)**. The SL output represented as fold change in GSL levels, showed that GSL production in these cells increased by 1.5-1.9 fold over control cells **(Fig.1E)**. Similarly, GSL output measured as GM/Gb ratio changed from 0.5 in control cells to 1.3 - 1.5 in treated cells **(Fig.1F)**. These data suggest that impaired spatial organization of enzymes correlates with altered SL output, and especially the output from steps involving competing reactions are sensitive to disorganization of the Golgi.

GRASP55 regulates SL output by controlling cargo flux between competing glycosylation pathways:

Retention of enzymes in the Golgi depends on their COPI dependent retrograde transport. Golgi matrix proteins especially Golgins contribute to specificity in this process (*23*) and thus to compartmentalization of enzymes. So, to identify specific regulators of compartmentalization of SL biosynthetic enzymes, we systematically silenced Golgi matrix proteins and studied the effect on SL production**.** Among the 15 matrix proteins tested by depletion, downregulation of GRASP55 significantly increased the production of GSLs (a 40% increase in GSLs compared to control) while downregulation of GOLPH3, GOPC and GCC2 led to a decrease in GSL levels **(Fig.2A)**. We followed up on GRASP55 since its depletion altered SL output similar to that obtained by disorganization of Golgi apparatus **(Fig.1E)**.

GRASP55 plays a role in stacking of Golgi *cis*ternae (*36, 37*), formation of Golgi ribbon (*38*), secretion (both conventional and unconventional) (*39-41*) and glycosylation (*42, 43*). We generated GRASP55 knockout (KO) HeLa cells (3 independent clones) using clustered regularly interspaced short palindromic repeat (CRISPR)/ CRISPR associated protein 9 (Cas9) technique **(Fig.S3A)** (see Methods). Western blotting and immunofluorescence confirmed the complete abolishment of GRASP55 expression in these KO clones **(Fig.S3B,C)** while expression levels of other Golgi matrix proteins were not altered **(Fig.S3D)**. Fragmentation of Golgi ribbon architecture was confirmed using both *cis* and *trans*- Golgi markers **(Fig.S4A-C)**. The Golgi stack itself did not reveal any obvious alterations **(Fig.S4D)**. Metabolic pulse chase experiments showed that biosynthesis of GSLs significantly increased in all three clones (by 30-50%) with a corresponding decrease in SM **(Fig.2B,S5A,B)** suggesting that there is bias towards SM production in the absence of GRASP55. The total levels of complex GSLs (GM, Gb) also increased and GM/Gb ratio was altered favouring ganglioside production in 2 out of 3 clones **(Fig.2C)**. The increased level of GSLs in cells is also evidenced by increased binding of bacterial toxins (shiga and cholera toxins that bind Gb3 and GM1 respectively) **(Fig.2D)** and by mass spectrometry analysis **(Fig.2E)**. A similar increase in GSL levels was also observed in GRASP55 KO human fibroblast cell line (Wi-26) **(Fig.S3E,S5C)**. Finally, the change in SL output associated with GRASP55 abolition was rescued by re-expressing GRASP55-GFP in these cell lines **(Fig.2B,S3C)** suggesting that the observed changes in GSLs were specific. We conclude that GRASP55 acts as a regulator of cargo flux at the two steps that involve competing reactions – SM *vs* GSLs and gangliosides *vs* globosides in the SL biosynthetic pathway.

GRASP55 regulates the intra-Golgi localization of GSL biosynthetic enzymes:

GRASP55 has been proposed to regulate glycosylation by regulating the kinetics of intra-Golgi transport (*42*) and/or ribbon formation (*43*). For GRASP55 mediated regulation of GSL biosynthesis, neither is a likely explanation since the kinetics of GSL biosynthesis **(Fig.S5A)** are very different from those of protein glycosylation (*42*) and downregulation of several matrix proteins known to fragment Golgi ribbon do not affect GSL biosynthesis **(Fig.2A)**. So, to understand how GRASP55 regulates GSL biosynthesis we first studied the consequences of GRASP55 deletion on SM biosynthetic machinery (ceramide transfer protein – CERT and SMS1). GRASP55 deletion did not reduce the levels of CERT or SMS1 **(Fig.S6A,B)**, alter their localization to Golgi **(Fig.S6C,D)** or change the dynamics of CERT **(Fig.S6D,E)**. The kinetics of

ceramide transport to Golgi also remained unaltered **(Fig.S6F)**. These data suggest that SM biosynthesis is not directly affected by GRASP55 deletion.

We next examined the effect of GRASP55 deletion on enzymes of the GSL biosynthetic branch. There were no consistent changes in their levels **(Fig.S7A)** or their presence in the Golgi **(Fig.S7B)** in GRASP55 KO cells. Their intra-Golgi localization was then examined in nocodazole-induced ministacks with GM130 as a marker for *cis*-Golgi/ *cis*-Golgi network (CGN) compartment and TGN46 as a marker for TGN (*44, 45*). The peak localization of GSL biosynthetic enzymes was found in the *medial/trans* part of Golgi in control cells **(Fig.S8)**. When GRASP55 was deleted the intra-Golgi localization of GlcCer synthase (GCS) and LacCer synthase (LCS) was shifted in the direction of *cis*-Golgi **(Fig.3A-B,S8A-B)** while the localization of SMS1, Gb3 synthase (Gb3S) and GM3 synthase (GM3S) was not altered **(Fig.S8C-E)**. The shift towards the *cis*-Golgi was also confirmed by electron microscopy. GCS which is localized mostly to *medial/trans*-Golgi (C3,C4 cisterna) with peak localization in C4 cisterna, was more equitably distributed across the stack in GRASP55 KO conditions **(Fig.3C,D)**. The *cis*-most cisterna (C1) which had minimal amount of GCS in control cells showed increased levels of GCS in GRASP55 KO cells, where it reached almost the same level as in other cisternae and in one clone (#2) even resulted in having the peak amount of enzyme **(Fig.3D)**. In case of LCS, there was a redistribution of the enzyme from *trans*-Golgi (C4 cisterna) to medial-Golgi (C2-C3 cisternae) in GRASP55 KO cells **(Fig.3C,E)**. Unlike GCS, LCS levels in the C1 cisterna did not change significantly **(Fig.3E)**. Thus, GRASP55 deletion changed the intra-Golgi localization of two key enzymes of GSL biosynthetic pathway *viz*. GCS and LCS, shifting them from their mainly *trans*-Golgi localization to more *cis/medial*-Golgi localization. While this change in localization co-occurs with the change in GSL biosynthesis, we wanted to explore if there exists a causal relation between these two phenomena. To achieve this, we engineered a change in localization of these enzymes without affecting GRASP55.

GRASP55 directly interacts with GCS and LCS to promote their sub-Golgi localization:

To engineer a change in localization of enzymes we first studied if and how GRASP55 interacts with GCS and LCS. We expressed GRASP55-GFP and HA-tagged versions of the GSL biosynthetic enzymes in HeLa cells, immunoprecipitated GRASP55-GFP and analysed for co-immunoprecipitation of HA-tagged enzymes by western blotting. We found that GRASP55-GFP specifically interacts with GCS and LCS but not with GM3S, which was used as a potential negative control **(Fig.4A,B).** This interaction is mediated through the cytosolic tails of these enzymes since the chemically synthesized cytosolic tails of GCS and LCS were able to “pull-

down" GRASP55 from HeLa cell cytosol **(Fig.4C,D)**. The cytosolic tails of GCS and LCS also interacted with purified His-tagged GRASP55 protein suggesting that the interaction was direct **(Fig.4E)**. There was no significant interaction (above background levels) of the peptides with GRASP65 **(Fig.4E)**, which is homologous to GRASP55, highlighting the specificity of the interaction. GRASP55 consists of two domains – an N-terminal tandem PDZ domains (GRASP domain) followed by a serine proline rich (*30*) (SPR) region. The cytosolic tails of GCS and LCS interacted with GST-tagged GRASP domain of GRASP55 and not with GST-tagged SPR region **(Fig.4F)**. GCS has a consensus class II PDZ domain interacting motif (Φ-X-Φ-COOH, where Φ refers to hydrophobic amino acid) LDV at the C-terminus. Deleting this motif in GCS cytosolic tail impaired its interaction with GRASP55 **(Fig.4D,G)** and an alanine scanning mutagenesis of LCS cytosolic tail revealed that the first 8 aminoacids are essential for GRASP55 interaction **(Fig.4D,H)**. Thus, GCS and LCS directly interact with the GRASP domain of GRASP55 **(Fig.4I)**. Next, we examined if binding to GRASP55 is essential for intra-Golgi localization of GCS and LCS. The last 3 C-terminal aminoacids of GCS and amino acids 2-10 of LCS were either deleted (GCS-Δ3C) or mutated to alanine (LCS9A) and their localization was studied. The intra-Golgi localization both GCS-Δ3C and LCS9A was altered, with both the constructs displaying a more *cis*-Golgi localization compared to WT enzymes **(Fig.4J,K)**. Thus, interaction with GRASP55 is essential for the correct sub-compartmentalization of GCS and LCS.

GRASP55 compartmentalizes LCS by promoting its anterograde transport:

Golgi localization of enzymes depends on their continuous retrograde flux mediated by COPI that opposes the anterograde flux of cargoes. To understand how GRASP55 acts to compartmentalize the enzymes, we chose to focus on LCS since we know more about the molecular mechanisms of Golgi retention of this protein which depends on COPI mediated retrograde transport promoted by GOLPH3 (*46*), a *trans*-Golgi localized protein. LCS localization is sensitive to the levels of GOLPH3. Decreasing GOLPH3 levels leads to the translocation of LCS from Golgi to the lysosomes **(Fig.S9)**, while increasing levels of GOLPH3 by overexpression leads to retrotranslocation of LCS to early compartments of the secretory pathway including the ER (*46*). Reduction in GRASP55 levels phenocopies to an extent the overexpression of GOLPH3, since LCS retrotranslocates to early Golgi under these conditions **(Fig.3B,C,E)**, suggesting that GRASP55 and GOLPH3 may contribute to opposing processes in the Golgi. So we examined the effects of overexpressing GRASP55. We co-transfected LCS and GRASP55-GFP in HeLa cells and the localization of LCS was monitored by immunofluorescence. When GRASP55 was overexpressed, there was a change in localization

of LCS, which was now present in endosome like structures along with the Golgi **(Fig.S9)**, qualitatively similar to what happens with GOLPH3 KD **(Fig.S9)** (*46*). This further strengthens the hypothesis that GOLPH3 and GRASP55 act in opposing manner on LCS. Next, we examined what happens if both GRASP55 and GOLPH3 are removed from the system. To this end, when both of them were removed by siRNA-mediated KD, LCS was found in endosome like structures **(Fig.S9)** similar to what happens in GOLPH3 KD cells **(Fig.S9)** (*46*). The dominance of GOLPH3 effects in this experiment, suggests that in the interaction between GRASP55 and GOLPH3, GOLPH3 likely acts downstream of GRASP55. To rationalize, these data into a model it is necessary to consider the localization of GRASP55 and GOLPH3. GRASP55 and GOLPH3 have not only opposing effects on the localization LCS, the localization of these proteins themselves is different. GRASP55 is mostly present in the early Golgi compartments with a peak localization to medial-Golgi and very little levels in the *trans*-Golgi (*36, 39*). On the other hand, GOLPH3 is mostly localized to *trans*-Golgi/TGN, with little if any protein in the *cis/medial*-Golgi (*46*). Based on this localization of GRASP55 and GOLPH3 and the above-discussed results, we propose the following model to explain the compartmentalization of LCS **(Fig.4L)**. When newly synthesized LCS enters the *cis*-Golgi it encounters predominantly GRASP55 over GOLPH3. We propose that GRASP55 promotes the anterograde transport of LCS in these compartments, likely by favouring the cisternal progression of the enzyme. When LCS reaches the *trans*-Golgi, the reduction in GRASP55 levels and increased levels of GOLPH3, lead to GOLPH3 taking over and promoting the COPI-mediated retrograde transport of LCS to maturing *medial*-cisternae, where it hands the baton back to GRASP55. A cyclical and balanced activity of GRASP55 and GOLPH3 ensues at this stage that compartmentalizes LCS to the *trans*-Golgi.

Change in intra-Golgi localization of GSL biosynthetic enzymes changes GSL output:

When GSL biosynthesis was examined in Brefeldin A treated cells, the increased GSL production of GRASP55 KO cells as well as their increased GM/Gb ratio was not observed **(Fig.5A,B)**, suggesting that compartmentalized localization of enzymes is essential to manifest GRASP55-deletion induced alteration in GSL production. Next, we examined GSL biosynthesis after expression of GCS and LCS mutants that have altered intra-Golgi localization. We expressed three GCS mutants: a. GCS-Δ3C that has more *cis*-Golgi presence than the WT enzyme **(Fig.4J)**, b. GCS with HA-tag at C-terminus (GCS-HA_C) that is expected to block accessibility to C-terminal Valine. GCS-HA_C distributes across the stack with significant presence in *cis*-Golgi (*30*) and unlike GCS-Δ3C it was also partially localized to ER **(Fig.S10)**

and c. GCS with HA-tag in N-terminus (GCS-HA_N), which localizes to ER **(Fig.S10)**. Thus, they have distinct but overlapping distribution along the secretory pathway. Expression of the wild type GCS construct in HeLa-M cells led to a 10% increase in the total GSLs produced compared to non-transfected cells suggesting that the expression of the construct does not overwhelm the biosynthetic system. The expression of GCS-Δ3C, which localizes to the *cis*-Golgi unlike wild type GCS, led to a 30% increase in GSLs produced, quantitatively similar to what is observed in GRASP55 KO cells, suggesting that the increased production of GSLs under GRASP55 KO conditions can be explained by the shift in localization of GCS. Interestingly, an increasingly ER localization of GCS (GCS-HA_C and GCS-HA_N) led to larger increase in GSL production (2.3 and 2.6-fold increase respectively) **(Fig.5C)**. The observed differences in GSL production are not due to differences in expression since addition of Brefeldin A neutralized these differences **(Fig.5C)**, implying that changes in localization were indeed the cause for observed increase in GSL production. Next, we manipulated the localization of LCS using *Retention using selective hooks* (RUSH; (*47*)) system. LCS WT and LCS9A constructs were expressed in HeLa LCS KO cells (*48*) and were either placed in ER or Golgi by selectively manipulating their exit out of ER (see Methods). Given that LCS acts at the bifurcation between the globoside and ganglioside biosynthesis, we studied the levels of complex GSLs in these cells. We found that the expression of LCS9A in Golgi favoured the production of gangliosides over globosides compared to LCS-WT. Thus GM/Gb ratio of 0.12 in case of LCS-WT expressing cells changed to 0.47 in case of LCS9A expressing cells **(Fig.5D)**. The differences were nullified when the enzymes were retained in ER **(Fig.5D)** suggesting that the observed differences were likely due to altered intra-Golgi localization of these enzymes. Thus, change in LCS localization observed in GRASP55 KO conditions may contribute to observed increase in GM/Gb ratio in these cells. From these data we conclude that change in GCS and LCS localization can reproduce the effects on SL biosynthesis following GRASP55 deletion and that localization of enzymes in the Golgi can control cargo flux across competing biosynthetic pathways.

To explain the effects of GRASP55 KO on GSL biosynthesis based on these results, we thus considered the localization of these respective enzymes. As discussed earlier, most of the GSL biosynthesis likely happens in the medial/*trans*-Golgi where along with the GSL enzymes a substantial portion of SMS1 is also located **(Fig.1B)**. This likely leads to a competition between SMS1 and GCS for Cer that is transported by vesicular transport to the *medial*/*trans*-Golgi **(Fig.5E)**. By moving GCS to the *cis*-Golgi, as happens in GRASP55 KO cells, the enzyme now gets a preferential access to Cer and resulting in an increased production of GSLs **(Fig.5E)**.

Indeed, in CERT KD cells where the non-vesicular transport of Cer is blocked and Cer reaches the Golgi mostly by vesicular transport, the effect on GSL biosynthesis resulting from the absence of GRASP55 is further increased **(Fig.5F)** suggesting the GCS and SMS1 compete for Cer that is transported by a vesicular transport pathway to the Golgi. Effect of GRASP55 KO on GSL output can also be explained by a similar logic. While both GM3S and Gb3S are localized mainly to the *medial/trans*-Golgi, significant amounts of GM3S can also be seen in *cis/medial*-Golgi unlike Gb3S **(Fig.S1)**. Thus, when LCS is moved towards the *cis/medial*-Golgi, ganglioside biosynthesis by GM3S is favoured over globoside biosynthesis likely due to preferential access of GM3S to the substrate LacCer.

Thus, these data provide a model of how compartmentalization of enzymes in the Golgi contributes to faithful glycan output. When two enzymes compete for a common substrate and are localized in the same compartment, the product of a glycoenzyme with more affinity for substrate and/or increased expression dominates the glycan output. On the contrary, if one of the competing enzymes is present in an earlier part of the secretory pathway relative to the other, it gets preferential access to the substrate before its competitor and thus promotes flux across the pathway catalysed by it resulting in a glycan output that has a bias towards product of this enzyme. Thus, positioning of enzymes in the Golgi regulates the pattern of glycan distribution in the output.

GRASP55 contributes to confluency induced changes in GSL production:

We then explored the physiological relevance of this GRASP55 mediated regulation of GSL biosynthesis. Confluence of fibroblasts is known to regulate GSL biosynthesis, which is required for cell density, induced contact inhibition of growth (*49*) and so we tested if this involves GRASP55-mediated regulation of GSL biosynthesis. We cultured human fibroblasts (wi-26) to different extents of confluence (25% to 100%) **(Fig.6A)** and monitored SL biosynthesis. A change in cell confluence was accompanied by a change in SL output. Going from sparse (25%) to complete confluence (100%), there was an increased production of SM with a corresponding decrease in GSL biosynthesis. SL output measured as GSL levels showed that there was an approximately 20% reduction in GSL production in completely confluent fibroblasts compared to sparse conditions **(Fig.6B)**. Next, we examined the reason behind the change in production of GSLs when cells reach confluence. It has been suggested that expression of GSL enzymes is altered with confluence (*49*). So, we analysed the levels of the SL biosynthetic enzymes in sparse and confluent cells by quantitative RT-PCR. As published earlier, we also found that the enzymes belonging to the distal end of GSL biosynthetic pathway namely GM2

synthase and GM1 synthase were increased in confluent cells compared to those grown under sparse conditions **(Fig.6C)**. Interestingly the enzymes of the early part of the SL biosynthetic pathway, namely the SMS1, GCS or LCS were not altered **(Fig.6C)** suggesting that the expression of key enzymes determining the proportion between SM and GSLs **(Fig.5C)** are not altered under these conditions. Since there is no change in the expression levels of key enzymes, we next examined whether a change in localization of enzymes could potentially underlie the change in GSL production. To this end, we studied the effect of addition of Brefeldin A that destroys enzyme organization **(Fig.S2)** on SL biosynthesis under both sparse and confluent conditions. We found that addition of Brefeldin A neutralizes the difference between sparse and confluent conditions with respect to GSL production **(Fig.6D)**, suggesting that the observed difference in GSL biosynthesis between sparse and confluent conditions is likely due to altered localization of SL biosynthetic enzyme(s). So, we examined the localization of GCS, the key enzyme that controls GSL production **(Fig.5C)** in sparse and confluent conditions. We found that GCS was mostly localized to the *trans*-Golgi in confluent conditions **(Fig.6E)** similar to what was observed earlier **(Fig.3)**, when cells were cultured in near confluent conditions (see Methods). On the contrary, in cells grown in sparse conditions, the peak localization of GCS was in the *cis*-side of the Golgi **(Fig.6E)**. These experiments together suggest that there is a difference in the localization of GCS between cells grown in sparse and confluence conditions and this likely accounts for the differences in SL biosynthesis in these cells. Then, we examined if GRASP55 contributes to this difference in localization of GCS and the subsequent change in SL biosynthesis between sparse and confluent fibroblasts. To this end, we first compared the localization of GCS in GRASP55 KO fibroblasts grown in sparse and confluent conditions. We found that in both these conditions, GCS was localized to the *cis*-side of the Golgi in GRASP55 KO fibroblasts **(Fig.6E)** similar to what was observed before in HeLa cells **(Fig.3)**. Next, we examined if there is a confluence-induced alteration in SL biosynthesis in GRASP55 KO fibroblasts. As noted earlier, GRASP55 KO fibroblasts produced more GSLs compared to control cells, **(Fig.S5C)** and these increased levels of GSLs were not reduced when cells reached complete confluence **(Fig.6F)**. This suggests that confluence associated reduction in GSL biosynthesis depends on GRASP55. These series of experiments suggest that when fibroblasts grow to reach confluence there is a GRASP55 dependent change in the localization of GCS from *cis*- to *trans*-Golgi and an associated reduction in GSL production.

Next, we explored if this GRASP55 mediated regulation of GSL biosynthesis that occurs when cells reach confluence is translated into observable cell behaviour. When cells reached complete confluence under *in vitro* culture conditions the phenomenon of contact inhibition of

growth is activated that prevents cell division. We examined if the absence of GRASP55 impaired contact inhibition of growth using focus-forming assay (*50*). Cells were cultured to complete confluence and maintained for 7-8 days before examining the number of foci formed. Control cells formed 4-5 foci per well, while GRASP55 KO cells had 4-fold more foci with 20-25 foci observed per well **(Fig.6G)**. To understand if this difference is due to altered GSL biosynthesis we studied the effect of inhibition of GSL biosynthesis on foci formation. The difference in number of foci was ablated upon treatment with 1-phenyl-2-decanoylamino-3-morpholino-1-propanol (PDMP) a known inhibitor of GSL biosynthesis **(Fig.6G)**. Thus, GRASP55 mediated reduction in GSL production associated with increased cell density contributes to contact inhibition of growth. Of note, increased GCS activity was correlated with tumour development in a mouse model of hepatocellular carcinoma (*51*) and mouse insertional mutagenesis studies have found that the inactivation of GRASP55 promotes tumour transformation and/or growth in liver and colorectal cancer models (Ref: Candidate Cancer Gene Database). In light of these observations, regulation of contact inhibition of growth by GRASP55 mediated alteration of GSL biosynthesis may have potential pathological relevance.

Discussion:

The molecular mechanisms of Golgi compartmentalization and its contribution to the regulation of glycosylation have remained fuzzy. We have identified for the first time a regulator of Golgi enzyme compartmentalization - GRASP55 that binds and compartmentalizes specific enzymes of the GSL biosynthetic pathway. While, studies on Golgi localization mechanisms have focused on retrograde transport pathway, surprisingly GRASP55 acts by promoting anterograde transport to compartmentalize the enzymes. The compartmentalization of enzymes mediated by GRASP55 controls the cargo flux between competing reactions by providing privileged access to the cargoes. Thus, GRASP55 controls the distribution of sphingolipids produced by the Golgi. We propose that transcriptional processes regulating the expression of glycosylation factors determine the type of glycans that will be produced, and membrane transport processes in the Golgi that regulate the levels (*52*) and localization of the enzymes determine the proportion of each glycoform produced. Thus, these two processes - transcriptional and Golgi membrane transport together define the glycan profile of a cell. We discuss below the implications of our study for the cell biology of Golgi organization as well as glycobiology.

Mechanisms regulating Golgi compartmentalization

Compartmentalization of Golgi residents is a dynamic process resulting from a balance between their anterograde and retrograde flux **(Fig.4L)**. According to the cisternal progression/maturation model, the anterograde flux is mediated by cisternal progression, a bulk-flow process and the retrograde flux by COPI mediated processes (*16, 17*). The mechanistic basis of retrograde transport is relatively well established with recent studies identifying specificity encoders in this transport process (*22-24, 46*). Here we discovered the existence of dedicated molecular machinery represented by GRASP55 that promotes the compartmentalized localization of certain enzymes by favouring their anterograde progression. Given GRASP55 controls the compartmentalization of only a sub-set of *trans*-Golgi residents, it likely does not influence the cisternal progression itself. If progression is a bulk-process, requirement for specific anterograde transporters is warranted only if at least some molecules can enter retrograde pathway in a signal-independent manner or with inappropriate exposition of signals. In which case, active mechanisms would be required to keep them from inappropriately entering retrograde transport. Interestingly Grasp proteins have been suggested to regulate COPI vesicle formation (*42, 53*) and our preliminary results indicate that absence of GRASP55 increases the presence of LCS and GCS in peri-Golgi vesicles. Thus, retrograde transport by COPI and cisternal progression, in some cases assisted by GRASP55, provide opposing forces to compartmentalize Golgi residents to specific cisternae. We also note that there are several other Golgi resident proteins with canonical PDZ domain binding motifs, which includes other enzymes and channels. Thus, GRASP55 (and possibly GRASP65) may play a wider role in the localization of several proteins in the Golgi.

Contribution of Golgi to fidelity of glycan biosynthesis:

The ordered arrangement of sequentially acting enzymes of N-glycan biosynthesis in Golgi implied that their localization might contribute to glycan output (*26*). Nonetheless, experiments have shown that a single compartment could still support sequential N-glycan processing (*54-57*). In retrospect, compartmentalization for sequentially acting enzymes seems superfluous. So, why did such elaborate organization of enzymes in the Golgi evolve? While the contribution of enzyme localization to the output of sequential reactions is not clear (but see (*58*)), the data presented here and by others (*59, 60*) clearly indicate that enzyme localization determines output of competing reactions. When two enzymes compete for a substrate, a privileged access to it (by differential positioning along the pathway) can increase the synthesis of glycans produced by the enzyme. While different from what is presented here, previous studies on

metabolic bias in sphingosine processing in lysosome *vs* mitochondria (*61*) and by Golgi to ER translocation of o-glycan initiating enzymes (*62*) suggest that localization-dependent regulation of glycosylation, and metabolism in general, may be a wide-spread phenomenon.

Regulation of glycosylation by GRASP55

GRASP55 has been suggested to play an important role in the stacking of cisternae (*36, 37*), formation of Golgi ribbon (*38*), conventional as well as unconventional secretion (*39-41*) and glycosylation (*42, 43*). It has been proposed to regulate glycosylation by regulating the kinetics of intra-Golgi transport (*42*) and/or ribbon formation (*43*). For GRASP55 mediated regulation of GSL biosynthesis, neither is a likely explanation since kinetics of GSL biosynthesis **(Fig.S5A)** is very different from that of protein glycosylation and downregulation of several matrix proteins known to fragment Golgi ribbon do not affect GSL biosynthesis **(Fig.2A)**. Instead, we show that absence of GRASP55 leads to a change in the localization of LCS and GCS **(Fig.3)**. This alters the SL production by providing a privileged early access of substrates to these enzymes and/or providing them a more permissive environment (*63, 64*) and thus increases GSL production **(Fig.5G)**. Thus, our study here provides an alternate or complementary view of how GRASP55 regulates glycosylation. Given the well-known regulation of GRASP55 activities by phosphorylation, we expect that GRASP55 mediated regulation of glycosylation by altering Golgi compartmentalization may turn out to be an important physiological phenomenon.

SL biosynthesis:

SL biosynthesis depends on CERT mediated transfer of ceramide from ER to TGN for SM biosynthesis (*65*) and FAPP2 mediated transfer of GlcCer from *cis*-Golgi to TGN for Gb3 biosynthesis (*29*). Earlier reports had shown that GCS and SMS1 are present in the *cis*- and *trans*-Golgi respectively (*30*). Surprisingly, we observe that GCS is present in the *medial/trans*-Golgi. We ascribe the observed difference in localization of GCS to the use of constructs with a tag that blocks the C-terminus (important for interaction with PDZ domain of GRASP55) in the previous studies (*30*). This revised localization of GCS has implications for the model of SL biosynthesis: if GCS is localized to *trans*-side why is the activity of GCS not sensitive to CERT KD? While GCS is indeed present in the *trans*-Golgi, SMS1 is present in a distinct compartment, the TGN. CERT mediated transfer of ceramide likely happens at the TGN and thus SMS1 depends on ceramide delivered by CERT unlike GCS.

To sum up, we identify a novel molecular pathway regulated by GRASP55 that compartmentalizes specific glycosylation enzymes and by this action modulates the competition between reactions to achieve a specific cellular glycan profile.

Acknowledgments

We thank Antonella De Matteis for valuable discussions, Nina Dathan for help with cloning and construct preparation and Francesco Russo for assistance with statistical analysis. We thank the Bioimaging Facility of the Institute of Protein Biochemistry and the FACS Facility of the Institute of Genetics and Biophysics (IGB-CNR, Naples) for access to technologies and Pasquale Barba assistance with FACS. We thank Drs. Corda, Colanzi, Grimaldi, Roy, Qadri, Krishnamoorthy, Ahamarshan and Polishchuk for critical comments. R.R. acknowledges financial support from Fondazione Italiana per la Ricerca sul Cancro (FIRC Fellowship 15111). A.L. acknowledges financial support from the Italian Cystic Fibrosis Research Foundation (Project #6), AIRC (Projects IG 15767 andIG 20786), the Italian Node of Euro-Bioimaging (Preparatory Phase II –INFRADEV), TERABIO the MIUR PON Project IMPARA and the POR Campania projects 2014-2020 C.I.R.O. and S.A.T.I.N. G.D.A. acknowledges financial support from EPFL institutional fund, Kristian Gerhard Jebsen Foundation and from the Swiss National Science Foundation (SNSF) (grant number, 310030_184926). S.P. acknowledges financial support from the Italian Cystic Fibrosis Research Foundation (Project #6), and the Italian Node of Euro-Bioimaging (Preparatory Phase II –INFRADEV).

Author contributions

PP contributed to development of the idea, conducted most of the experiments, analysis and interpretation of data and contributed to writing the manuscript; IA conducted the experiments on peptide binding using purified proteins; MP was involved in labelling and acquisition of EM and confocal microscopy images; RR conducted experiments on double knockdown and assisted in acquisition of electron micrographs; DR conducted mRNA analysis; GT was involved in EM sample preparation and acquisition of images; LC conducted MALDI-MS and lipidomics measurements; GV assisted PP in morphological analysis of Golgi; ND was involved in cloning and construct preparation; PH was involved in synthesis of biotinylated peptides; JN and MP provided the WT and GRASP55 KO fibroblasts; MJH, LO and YH contributed to MS analysis of lipids. AL and GDA contributed to development of the idea, critical analysis of the data throughout the entire project and also provided critical inputs in manuscript preparation. SP developed the idea, designed and supervised the entire project, and wrote the manuscript.

Conflicts of interest

The authors declare no potential conflicts of interest.

Reference:

1. A. Kohyama-Koganeya, T. Nabetani, M. Miura, Y. Hirabayashi, Glucosylceramide synthase in the fat body controls energy metabolism in Drosophila. *J Lipid Res* **52**, 1392-1399 (2011).
2. M. C. Ryczko *et al.*, Metabolic Reprogramming by Hexosamine Biosynthetic and Golgi N-Glycan Branching Pathways. *Sci Rep* **6**, 23043 (2016).
3. A. Akintayo, P. Stanley, Roles for Golgi Glycans in Oogenesis and Spermatogenesis. *Front Cell Dev Biol* **7**, 98 (2019).
4. J. R. Bishop, M. Schuksz, J. D. Esko, Heparan sulphate proteoglycans fine-tune mammalian physiology. *Nature* **446**, 1030-1037 (2007).
5. A. Varki, Biological roles of glycans. *Glycobiology* **27**, 3-49 (2017).
6. D. Russo *et al.*, Glycosphingolipid metabolic reprogramming drives neural differentiation. *EMBO J* **37**, (2018).
7. I. J. Chang, M. He, C. T. Lam, Congenital disorders of glycosylation. *Ann Transl Med* **6**, 477 (2018).
8. P. Stanley, Golgi glycosylation. *Cold Spring Harb Perspect Biol* **3**, (2011).
9. A. Varki, S. Kornfeld, in *Essentials of Glycobiology,* rd *et al.*, Eds. (Cold Spring Harbor (NY), 2015), pp. 1-18.
10. P. Rudd, N. G. Karlsson, K. H. Khoo, N. H. Packer, in *Essentials of Glycobiology,* rd *et al.*, Eds. (Cold Spring Harbor (NY), 2015), pp. 653-666.
11. A. V. Nairn *et al.*, Regulation of glycan structures in murine embryonic stem cells: combined transcript profiling of glycan-related genes and glycan structural analysis. *J Biol Chem* **287**, 37835-37856 (2012).
12. A. V. Nairn *et al.*, Regulation of glycan structures in animal tissues: transcript profiling of glycan-related genes. *J Biol Chem* **283**, 17298-17313 (2008).
13. H. J. Maccioni, C. G. Giraudo, J. L. Daniotti, Understanding the stepwise synthesis of glycolipids. *Neurochem Res* **27**, 629-636 (2002).
14. A. Varki, Factors controlling the glycosylation potential of the Golgi apparatus. *Trends Cell Biol* **8**, 34-40 (1998).
15. J. Klumperman, Architecture of the mammalian Golgi. *Cold Spring Harb Perspect Biol* **3**, (2011).
16. B. S. Glick, A. Luini, Models for Golgi traffic: a critical assessment. *Cold Spring Harb Perspect Biol* **3**, a005215 (2011).
17. A. Nakano, A. Luini, Passage through the Golgi. *Curr Opin Cell Biol* **22**, 471-478 (2010).
18. M. Ishii, Y. Suda, K. Kurokawa, A. Nakano, COPI is essential for Golgi cisternal maturation and dynamics. *J Cell Sci* **129**, 3251-3261 (2016).
19. E. Papanikou, K. J. Day, J. Austin, B. S. Glick, COPI selectively drives maturation of the early Golgi. *Elife* **4**, (2015).
20. V. Popoff, F. Adolf, B. Brugger, F. Wieland, COPI budding within the Golgi stack. *Cold Spring Harb Perspect Biol* **3**, a005231 (2011).
21. C. Rabouille, J. Klumperman, Opinion: The maturing role of COPI vesicles in intra-Golgi transport. *Nat Rev Mol Cell Biol* **6**, 812-817 (2005).
22. L. Liu, B. Doray, S. Kornfeld, Recycling of Golgi glycosyltransferases requires direct binding to coatomer. *Proc Natl Acad Sci U S A* **115**, 8984-8989 (2018).
23. M. Wong, S. Munro, Membrane trafficking. The specificity of vesicle traffic to the Golgi is encoded in the golgin coiled-coil proteins. *Science* **346**, 1256898 (2014).
24. E. S. Eckert *et al.*, Golgi phosphoprotein 3 triggers signal-mediated incorporation of glycosyltransferases into coatomer-coated (COPI) vesicles. *J Biol Chem* **289**, 31319-31329 (2014).
25. J. B. Blackburn, Z. D'Souza, V. V. Lupashin, Maintaining order: COG complex controls Golgi trafficking, processing, and sorting. *FEBS Lett* **593**, 2466-2487 (2019).

26. W. G. Dunphy, J. E. Rothman, Compartmental organization of the Golgi stack. *Cell* **42**, 13-21 (1985).
27. P. Pothukuchi *et al.*, Translation of genome to glycome: role of the Golgi apparatus. *FEBS Lett* **593**, 2390-2411 (2019).
28. M. T. Anjali Jaiman, Algorithmic biosynthesis of eukaryotic glycans. *Bioarxiv*, (2018).
29. G. D'Angelo *et al.*, Vesicular and non-vesicular transport feed distinct glycosylation pathways in the Golgi. *Nature* **501**, 116-120 (2013).
30. D. Halter *et al.*, Pre- and post-Golgi translocation of glucosylceramide in glycosphingolipid synthesis. *J Cell Biol* **179**, 101-115 (2007).
31. Y. A. Hannun, L. M. Obeid, Sphingolipids and their metabolism in physiology and disease. *Nat Rev Mol Cell Biol* **19**, 175-191 (2018).
32. D. Russo, L. Capolupo, J. S. Loomba, L. Sticco, G. D'Angelo, Glycosphingolipid metabolism in cell fate specification. *J Cell Sci* **131**, (2018).
33. S. Parashuraman, G. D'Angelo, Visualizing sphingolipid biosynthesis in cells. *Chem Phys Lipids* **218**, 103-111 (2019).
34. M. Aridor, S. I. Bannykh, T. Rowe, W. E. Balch, Sequential coupling between COPII and COPI vesicle coats in endoplasmic reticulum to Golgi transport. *J Cell Biol* **131**, 875-893 (1995).
35. C. J. Zhang *et al.*, Expression of a dominant allele of human ARF1 inhibits membrane traffic in vivo. *J Cell Biol* **124**, 289-300 (1994).
36. J. Shorter *et al.*, GRASP55, a second mammalian GRASP protein involved in the stacking of Golgi cisternae in a cell-free system. *EMBO J* **18**, 4949-4960 (1999).
37. Y. Xiang, Y. Wang, GRASP55 and GRASP65 play complementary and essential roles in Golgi cisternal stacking. *J Cell Biol* **188**, 237-251 (2010).
38. T. N. Feinstein, A. D. Linstedt, GRASP55 regulates Golgi ribbon formation. *Mol Biol Cell* **19**, 2696-2707 (2008).
39. G. D'Angelo *et al.*, GRASP65 and GRASP55 sequentially promote the transport of C-terminal valine-bearing cargos to and through the Golgi complex. *J Biol Chem* **284**, 34849-34860 (2009).
40. M. Chiritoiu, N. Brouwers, G. Turacchio, M. Pirozzi, V. Malhotra, GRASP55 and UPR Control Interleukin-1beta Aggregation and Secretion. *Dev Cell* **49**, 145-155 e144 (2019).
41. J. Kim *et al.*, Monomerization and ER Relocalization of GRASP Is a Requisite for Unconventional Secretion of CFTR. *Traffic* **17**, 733-753 (2016).
42. Y. Xiang *et al.*, Regulation of protein glycosylation and sorting by the Golgi matrix proteins GRASP55/65. *Nat Commun* **4**, 1659 (2013).
43. T. Jarvela, A. D. Linstedt, Isoform-specific tethering links the Golgi ribbon to maintain compartmentalization. *Mol Biol Cell* **25**, 133-144 (2014).
44. G. V. Beznoussenko *et al.*, Transport of soluble proteins through the Golgi occurs by diffusion via continuities across cisternae. *Elife* **3**, (2014).
45. R. Rizzo *et al.*, The dynamics of engineered resident proteins in the mammalian Golgi complex relies on cisternal maturation. *J Cell Biol* **201**, 1027-1036 (2013).
46. D. R. Riccardo Rizzo, Kazuo Kurokawa, Pranoy Sahu, Bernadette Lombardi, Domenico Supino, Mikhail Zhukovsky, Anthony Vocat, Prathyush Pothukuchi, Vidya Kunnathully, Laura Capolupo, Gaelle Boncompain, Carlo Vitagliano, Federica Zito Marino, Gabriella Aquino, Daniela Montariello, Petra Henklein, Luigi Mandrich, Gerardo Botti, Henrik Clausen, Ulla Mandel, Toshiyuki Yamaji, Kentaro Hanada, Alfredo Budillon, Franck Perez, Seetharaman Parashuraman, Yusuf A Hannun, Akihiko Nakano, Daniela Corda, Giovanni D'Angelo, Alberto Luini, The Glyco-enzyme adaptor GOLPH3 Links Intra-Golgi Transport Dynamics to Glycosylation Patterns and Cell Proliferation. *Bioarxiv*, (2019).

641 47. G. Boncompain *et al.*, Synchronization of secretory protein traffic in populations of cells. *Nat*
642 *Methods* **9**, 493-498 (2012).
643 48. T. Yamaji, K. Hanada, Establishment of HeLa cell mutants deficient in sphingolipid-related genes
644 using TALENs. *PLoS One* **9**, e88124 (2014).
645 49. X. Huang, N. Schurman, K. Handa, S. Hakomori, Functional role of glycosphingolipids in contact
646 inhibition of growth in a human mammary epithelial cell line. *FEBS Lett* **591**, 1918-1928 (2017).
647 50. A. Alvarez, G. A. Barisone, E. Diaz, Focus formation: a cell-based assay to determine the
648 oncogenic potential of a gene. *J Vis Exp*, (2014).
649 51. Y. Guri *et al.*, mTORC2 Promotes Tumorigenesis via Lipid Synthesis. *Cancer Cell* **32**, 807-823 e812
650 (2017).
651 52. D. R. Riccardo Rizzo, Kazuo Kurokawa, Pranoy Sahu, Bernadette Lombardi, Domenico Supino,
652 Mikhail Zhukovsky, Anthony Vocat, Prathyush Pothukuchi, Vidya Kunnathully, Laura Capolupo,
653 Gaelle Boncompain, Carlo Vitagliano, Federica Zito Marino, Gabriella Aquino, Petra Henklein,
654 Luigi Mandrich, Gerardo Botti, Henrik Clausen, Ulla Mandel, Toshiyuki Yamaji, Kentaro Hanada,
655 Alfredo Budillon, Franck Perez, Seetharaman Parashuraman, Yusuf A Hannun, Akihiko Nakano,
656 Giovanni D'Angelo, Alberto Luini, Retrograde Transport of Golgi Enzymes by GOLPH3 Across
657 Maturing Cisternae Regulates Glycan Assembly on Sphingolipids and Cell Growth. *Bioarxiv*,
658 (2019).
659 53. T. V. Rianne Grond, Juan Duran, Ishier Raote, Sebastiaan Corstjens, Laura Delfgou, Benaissa El
660 Haddouti, Vivek Malhotra, Catherine Rabouille, GORASPs link Golgi cisternae laterally to stabilize
661 the rims and prevent vesiculation. *Bioarxiv*, (2020).
662 54. N. W. Chege, S. R. Pfeffer, Compartmentation of the Golgi complex: brefeldin-A distinguishes
663 trans-Golgi cisternae from the trans-Golgi network. *J Cell Biol* **111**, 893-899 (1990).
664 55. B. K. Hayes, H. H. Freeze, A. Varki, Biosynthesis of oligosaccharides in intact Golgi preparations
665 from rat liver. Analysis of N-linked glycans labeled by UDP-[6-3H]N-acetylglucosamine. *J Biol*
666 *Chem* **268**, 16139-16154 (1993).
667 56. L. Karhinen, M. Makarow, Activity of recycling Golgi mannosyltransferases in the yeast
668 endoplasmic reticulum. *J Cell Sci* **117**, 351-358 (2004).
669 57. S. Kim, Y. Miura, J. R. Etchison, H. H. Freeze, Intact Golgi synthesize complex branched O-linked
670 chains on glycoside primers: evidence for the functional continuity of seven glycosyltransferases
671 and three sugar nucleotide transporters. *Glycoconj J* **18**, 623-633 (2001).
672 58. P. Fisher, H. Spencer, J. Thomas-Oates, A. J. Wood, D. Ungar, Modeling Glycan Processing
673 Reveals Golgi-Enzyme Homeostasis upon Trafficking Defects and Cellular Differentiation. *Cell*
674 *Rep* **27**, 1231-1243 e1236 (2019).
675 59. E. Grabenhorst, H. S. Conradt, The cytoplasmic, transmembrane, and stem regions of
676 glycosyltransferases specify their in vivo functional sublocalization and stability in the Golgi. *J*
677 *Biol Chem* **274**, 36107-36116 (1999).
678 60. D. Skrincosky *et al.*, Altered Golgi localization of core 2 beta-1,6-N-acetylglucosaminyltransferase
679 leads to decreased synthesis of branched O-glycans. *J Biol Chem* **272**, 22695-22702 (1997).
680 61. S. Feng *et al.*, Lysosome-targeted photoactivation reveals local sphingosine metabolism
681 signatures. *Chem Sci* **10**, 2253-2258 (2019).
682 62. F. Bard, J. Chia, Cracking the Glycome Encoder: Signaling, Trafficking, and Glycosylation. *Trends*
683 *Cell Biol* **26**, 379-388 (2016).
684 63. Y. Hayashi *et al.*, Complex formation of sphingomyelin synthase 1 with glucosylceramide
685 synthase increases sphingomyelin and decreases glucosylceramide levels. *J Biol Chem* **293**,
686 17505-17522 (2018).
687 64. Y. Ishibashi, M. Ito, Y. Hirabayashi, Regulation of glucosylceramide synthesis by Golgi-localized
688 phosphoinositide. *Biochem Biophys Res Commun* **499**, 1011-1018 (2018).

689 65. K. Hanada *et al.*, Molecular machinery for non-vesicular trafficking of ceramide. *Nature* **426**,
690 803-809 (2003).

691

692

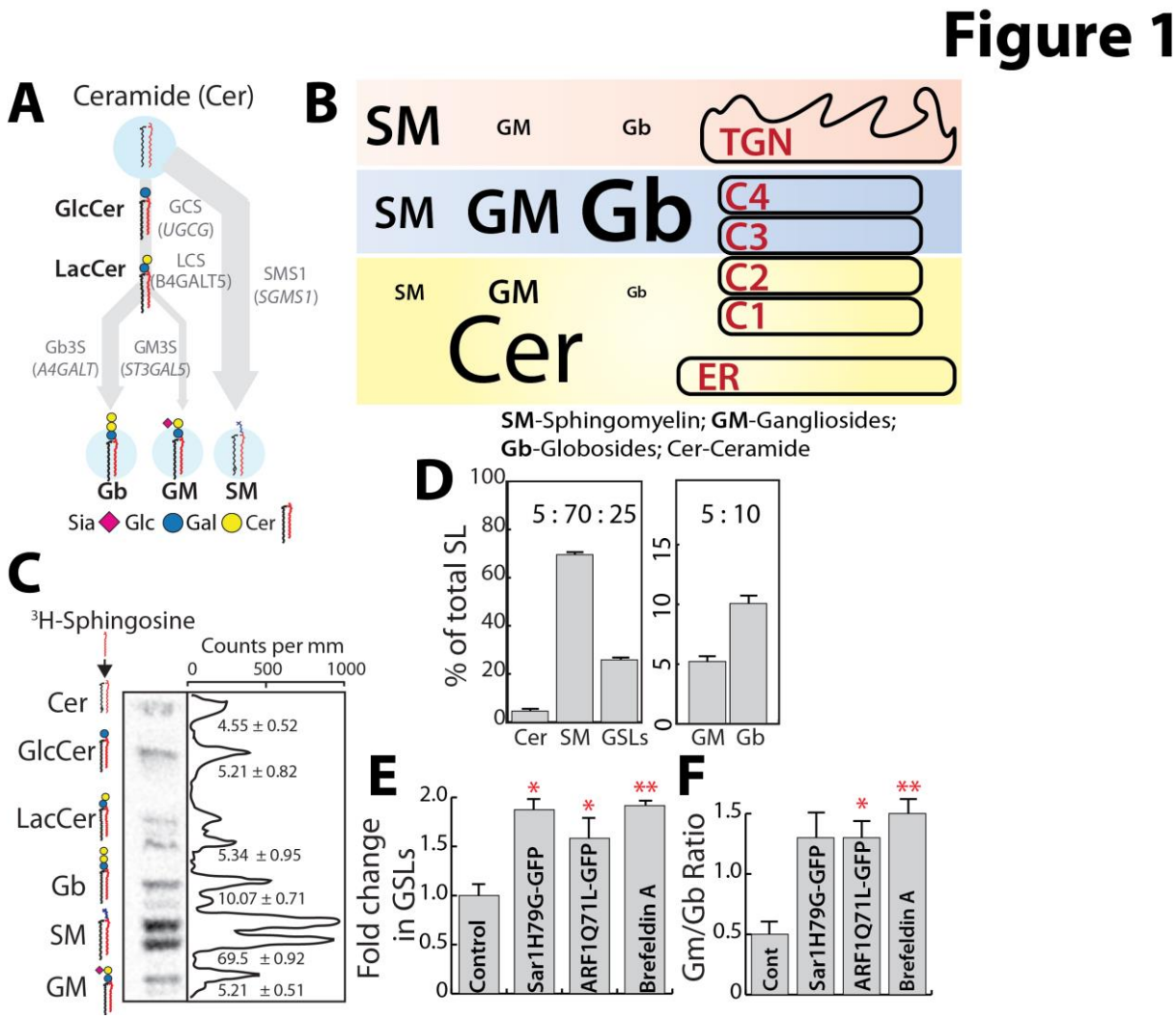

Figure 1. Disruption of SL biosynthetic machinery organization alters SL output:

(A) Schematic representation of GSL biosynthetic pathway in HeLa cells (Glc, glucose; Gal, galactose; Sia, N-acetylneuraminicacid; Cer, ceramide). Products of biosynthesis are represented in bold and enzymes which catalyse the reactions in grey. The arrows represent the SL metabolic flux from ceramide. **(B)** Schematic representation of GSL biosynthetic zones in HeLa, SM biosynthesis predominates in TGN, whereas GSL and SM production happens in *medial/trans*-Golgi (C3 and C4 cisternae). Cis-Golgi/ER is where Ceramide biosynthesis happens with little if any SL production. The size of the lipid label represents the proportion of the lipid expected to be synthesized in a compartment based on the localization of corresponding enzymes **(C)** High-performance thin-layer chromatography (HPTLC) profile of HeLa cells pulsed for 2 hours with [^{3}H]-sphingosine and chased for 24 hours. The peaks corresponding to each SL species is indicated and numbers represent each SL species as percentage of total SL. **(D)** The total radioactivity associated with Cer, SM and GSLs (GluCer,

LacCer, Gb and GM) or GM and Gb was quantified and presented as percentages relative to total. Data represented as means ± SD of 3 independent experiments. **(E-F)** Biosynthesis of SL in HeLa cells expressing GTP locked mutants of Sar1 or ARF1 or treated with brefeldin A (BFA) (5µg/ml) was measured by [^{3}H] - sphingosine pulse-chase assay. Relative radioactivity associated with Cer, SM and GSLs were quantified and represented as fold change with respect to control. **(E)** The ratio of GM/Gb is represented. **(F)** For BFA treated cells, the SL output was measured 8h after pulse. Data represented as means ± SD of 2 independent experiments. *P< 0.05, **P<0.01 (Student's t test).

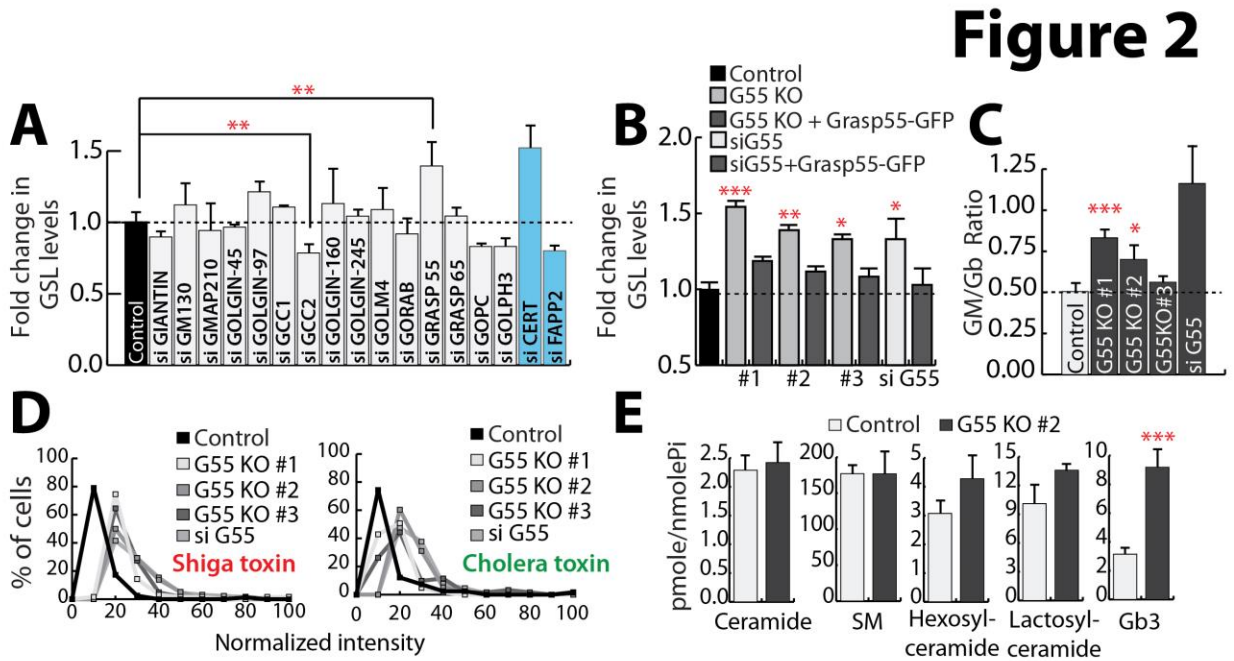

Figure 2. GRASP55 regulates SL biosynthesis:

(A) HeLa cells were treated with control or indicated siRNA (pool of 4 or 2 as indicated in methods) for 72 hours and SL biosynthesis measured by [^{3}H] - sphingosine pulse-chase assay. GSL levels are expressed as fold changes with respect to control. CERT and FAPP2 knockdowns were used as positive and negative controls respectively. **(B-C)** Effect of GRASP55 depletion on SL biosynthesis monitored by [^{3}H] - sphingosine pulse-chase assay in GRASP55 KO cells or cells treated with GRASP55 siRNA or following expression of GRASP55-GFP in GRASP55 depleted cells. GSL levels are expressed as fold changes respect to control. **(C)** The levels of GM and Gb were quantified and represented as ratio of GM/Gb ratio. **(D)** Effect of GRASP55 depletion on GSL levels measured by Cy3-conjugated ShTxB (Shiga Toxin) and Alexa488-conjugated ChTxB (Cholera Toxin) staining in control and GRASP 55 KO cells or cells treated with GRASP55 siRNA. Frequency distribution of level of STxB and CTxB staining is represented with intensities normalized to maximum intensity for each condition (>100 cells per condition were analysed). **(E)** SL levels as assessed by LC/MS or MALDI-MS (Gb3) in control and GRASP55 KO (#2) cells. Data represented are mean ± SD of 3 independent experiments *p <0.05, **p <0.01, ***p <0.001 (Student's t test).

Figure 3

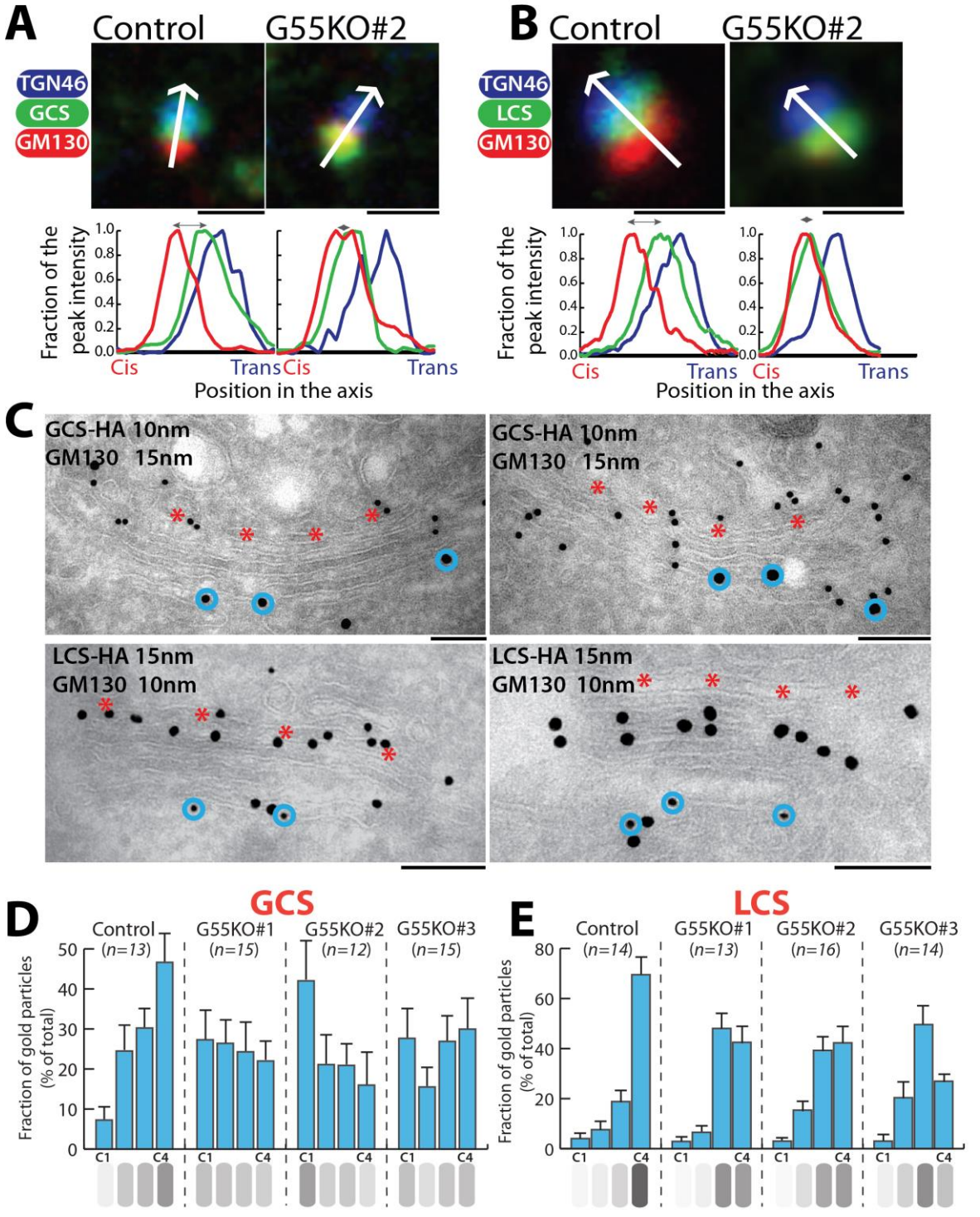
A
Control
G55KO#2
TGN46
GCS
GM130
Fraction of the peak intensity
Cis
Trans
Position in the axis
B
Control
G55KO#2
TGN46
LCS
GM130
Fraction of the peak intensity
Cis
Trans
Position in the axis
C
GCS-HA 10nm
GM130 15nm
LCS-HA 15nm
GM130 10nm
D
GCS
Control (n=13)
G55KO#1 (n=15)
G55KO#2 (n=12)
G55KO#3 (n=15)
Fraction of gold particles (% of total)
C1
C4
E
LCS
Control (n=14)
G55KO#1 (n=13)
G55KO#2 (n=16)
G55KO#3 (n=14)
Fraction of gold particles (% of total)
C1
C4

733

Figure 3. GRASP55 regulates the intra-Golgi localization of GSL biosynthetic enzymes:

(A-B) Control and GRASP55 KO clones were transfected with HA-tagged GSL biosynthetic enzymes, treated with nocodazole (33 µM) for 3 hours, and processed for immunofluorescence with anti-HA (green), anti-GM130 (red), and anti-TGN46 (blue) antibodies. The relative position of HA-tagged enzymes with respect to GM130 and TGN46 was measured by line scanning and expressed as normalized positions of the peak intensity with the start of GM130 peak indicated as Cis and the end of TGN46 peak indicated as trans in the graph. Scale Bar 1µm. **(C)** Control and GRASP55 KO cells were transfected for 16 hours with GCS-HA or LCS-HA and processed for cryoimmunolabeling with anti-HA antibody (10-nm gold particles) and anti-GM130 antibody (15-nm gold particles) in case of GCS-HA and anti-HA antibody (15-nm gold particles) and anti-GM130 antibody (10-nm gold particles) in case of LCS-HA . Representative images of the distribution of GCS-HA and LCS-HA are shown. Bar 200nm. Red asterisk marks C4 cisterna and blue circles indicate GM130 labelling. **(D-E)** Distribution of indicated enzymes across the Golgi stack was quantified and represented as fraction of Gold particles in each cisternae for GCS-HA **(D)** and LCS- HA **(E)** (n indicated in the graph; data are Mean ± SEM).

Figure 4

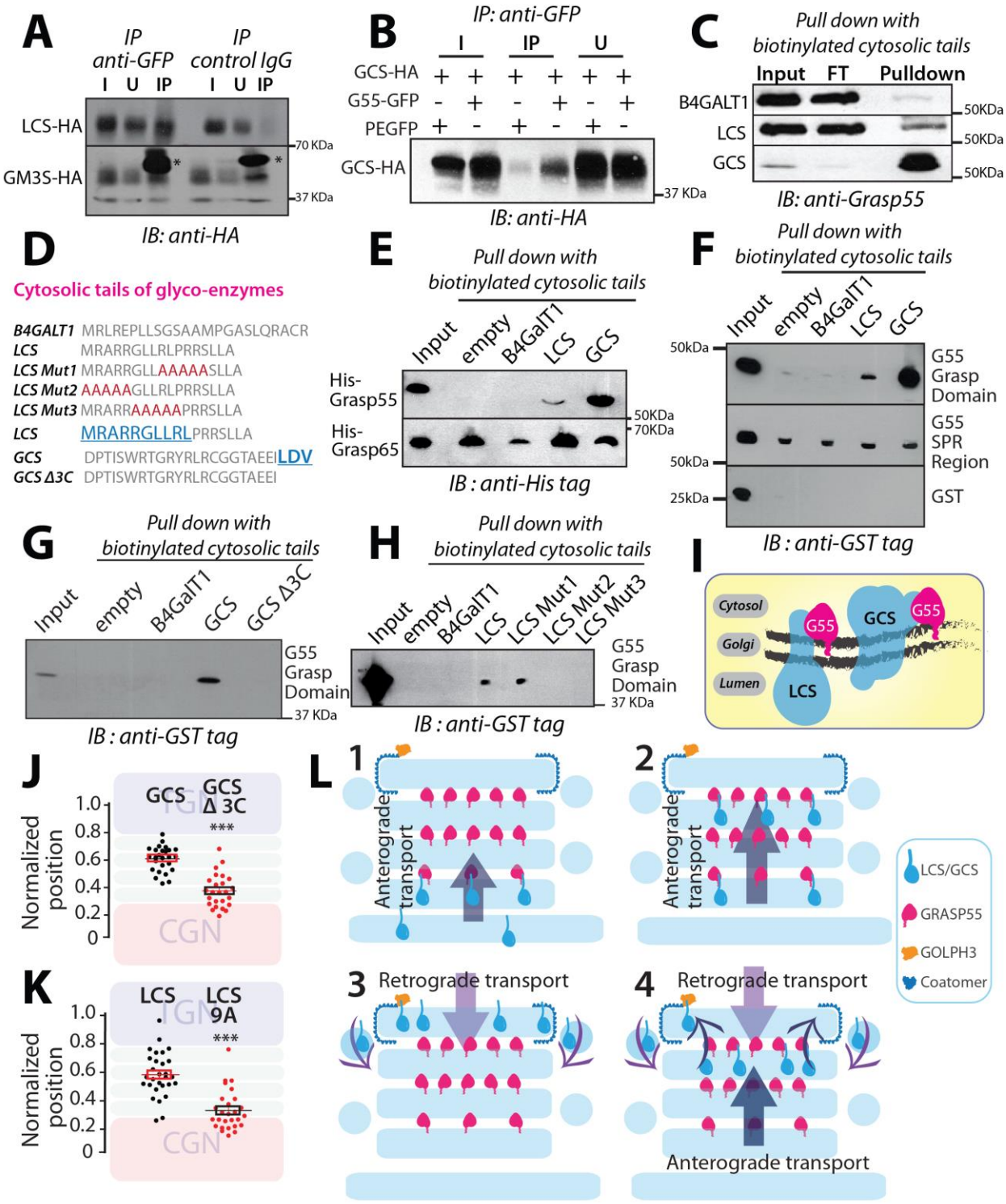

750
751

Figure 4. GRASP55 directly interacts with GCS and LCS to promote their sub-Golgi localization:

(A) HeLa cells co-transfected with indicated HA tagged enzymes (LCS and GM3S) and GRASP55-GFP were lysed, immunoprecipitated with anti-GFP antibody or control IgG and were analysed by western blotting for interaction by immunoblotting (IB) with anti-HA antibody. I represents 5% on the input lysate, U 5% of the unbound fraction and IP the immunoprecipitate. Asterisks indicate IgG band **(B)** HeLa cells co-transfected with HA tagged GCS and GRASP55-GFP or empty vector (pEGFP) were lysed, immunoprecipitated with anti-GFP antibody and analysed by western blotting for interaction by immunoblotting (IB) with anti-HA antibody. Legends as described in (**A**). **(C)** Chemically synthesized biotinylated peptides corresponding to cytosolic portions of glycosylation enzymes were used to pull down interactors from HeLa cell lysates and subjected to immunoblotting with anti-GRASP55 antibodies. **(D)** Represents the amino acid sequence of cytosolic tails of indicated glycosylation enzymes. Potential sites on the cytosolic tails of enzymes for GRASP55 binding are indicated in blue and red indicates Alanine substitution of corresponding aminoacids in WT cytoplasmic tails. **(E-H)** Chemically synthesized biotinylated peptides corresponding to cytosolic portions of glycosylation enzymes and indicated purified His-tagged GRASP65 full-length, GRASP55 full-length, GST-tagged GRASP domain and SPR region of GRASP55 were incubated together and their interaction was monitored by pulling down the biotinylated peptides with avidin beads followed by western blotting with anti-His tag or anti-GST tag antibody as indicated. **(I)** Model representing the interaction between GRASP55 and the cytosolic tails of GCS and LCS. **(J-K)** HeLa cells were transfected with either WT GCS, LCS or indicated mutants, treated with nocodazole (33 µM) for 3 hours and labelled for enzymes, GM130, and TGN46. Line scan analysis was performed as in Fig.3A-B and the relative position of enzymes was quantitated and plotted. The data are mean ± SD; n> 30 stacks. ***p <0.001(Student's t test). **(L)** Model represents GRASP55 mediated compartmentalization of GCS and LCS. 1 and 2. The newly synthetized (LCS /GCS; blue) arrives at the *cis*-Golgi from ER and encounters GRASP55 (pink), which promotes the anterograde movement of the enzymes. 3. The enzyme (LCS/GCS) thus reaches the *trans*-Golgi, where it is retrogradely transported by COPI, in some cases assisted by adaptor proteins (GOLPH3;orange). 4. A cyclical and balanced activity of GRASP55 and GOLPH3 ensues at this stage that compartmentalizes LCS to the *trans*-Golgi. Thus anterograde transport of enzymes (indicated in blue) counterbalance their retrograde transport (indicated in purple) resulting in the compartmentalization of these enzymes.

Figure 5

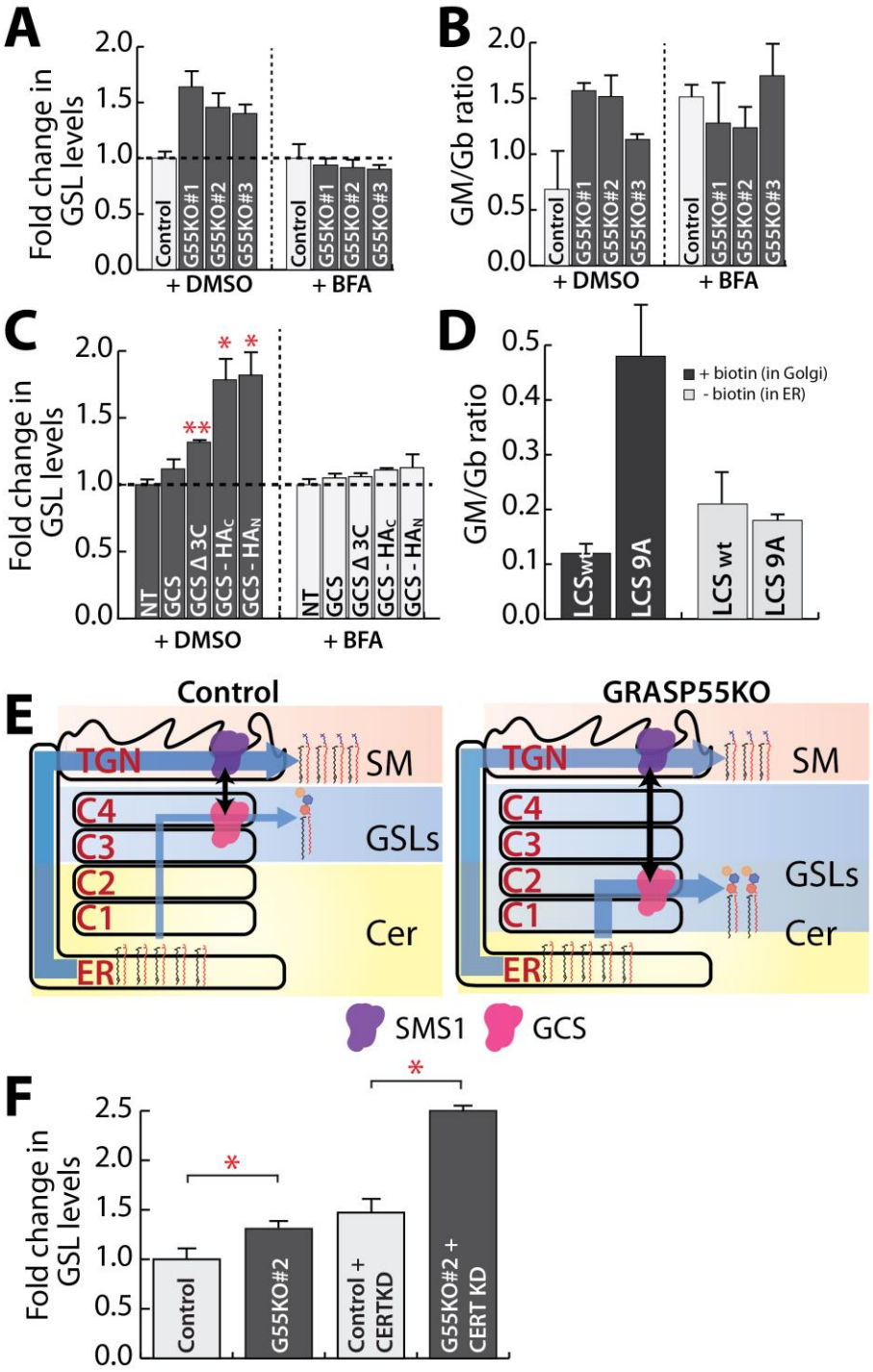
A
Fold change in GSL levels
2.0
1.5
1.0
0.5
0.0
Control
G55KO#1
G55KO#2
G55KO#3
+ DMSO
+ BFA
B
GM/Gb ratio
C
NT
GCS
GCS Δ 3C
GCS - HAC
GCS - HAN
D
+ biotin (in Golgi)
- biotin (in ER)
LCSwt
LCS 9A
LCS wt
E
Control
GRASP55KO
TGN
SM
C4
C3
C2
C1
GSLs
Cer
ER
SMS1
GCS
F
G55KO#2
Control + CERTKD
G55KO#2 + CERT KD

785

Figure 5. Change in intra-Golgi localization of GSL biosynthetic enzymes changes GSL output:

(A-B) Control and GRASP55 KO clones were pre-treated with DMSO or BFA (5µg/ml) for 30 min and SL output monitored by [^{3}H] - sphingosine pulse-chase assay (8 h chase). **(A)** Total GSL levels were quantified and expressed as fold changes with respect to control. **(B)** The ratio of GM/Gb calculated and represented. Data are mean ± SD of 2 independent experiments. **(C)** HeLa cells were transfected with indicated GCS constructs for 16 hours and SL output monitored by [^{3}H] - sphingosine pulse-chase assay (8 h chase) in the presence or absence of BFA (5µg/ml). Total GSL levels were quantified and expressed as fold changes respect to control. Data are mean ± SD of 2 independent experiments. **(D)** HeLa cells KO for LCS were transfected with indicated LCS RUSH constructs for 16 hours, and expressed enzymes were retained in the ER (-biotin) or placed in the Golgi by addition of biotin (40 µM) (+biotin) and SL output monitored by [^{3}H] - sphingosine pulse-chase assay. The ratio of GM/Gb is represented. Data are mean ± SD of 2 independent experiments. **(E)** Schematic representation of how the change in localization of GCS (pink) from *trans*- to *cis*-Golgi results in preferential access to ceramide and thus an increased production of GSLs. The flux of ceramide is represented by blue arrow. **(F)** CERT was silenced using siRNAs for 72 hours in control and GRASP55 KO(#2) clone before subjecting to [^{3}H] –sphingosine pulse chase assay. GSLs were quantified and represented as fold change with respect to control. Values are mean ± SD (n=3).

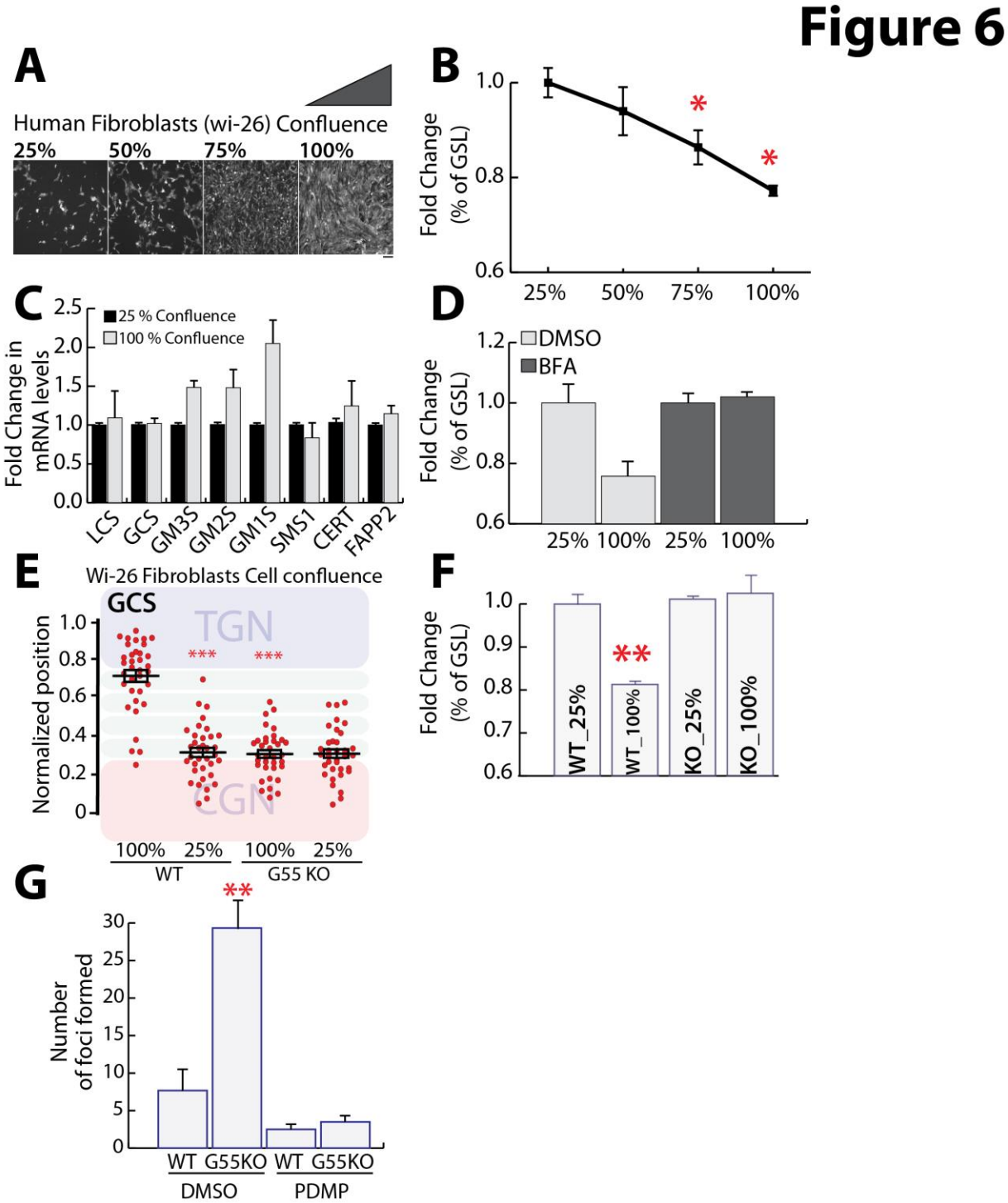

806 **Figure 6. GRASP55 contributes to confluency induced changes in GSL production:**

807 **(A)** Fibroblasts were grown to indicated confluency and imaged. Scale bar, 100um. **(B)**
808 Fibroblasts were grown to indicated confluency and SL output monitored by [^{3}H] - sphingosine
809 pulse-chase assay. Total GSL levels was quantified and represented as fold changes with

respect to lowest confluence (25%). **(C)** Fibroblasts were grown to complete confluence or sparse (25% confluence), mRNAs were extracted and indicated mRNAs were quantified by RT-PCR and expressed as levels relative to those in cells grown in sparse condition. **(D)** Fibroblasts were grown to complete confluence or sparse (25% confluence), treated with DMSO or Brefeldin A (5µg/ml) for 30min and SL production monitored by [^{3}H] - sphingosine pulse-chase assay in the continued presence of DMSO or Brefeldin A for 8h. Total GSL levels was quantified and represented as fold changes respect to lowest confluence (25%). **(E)** Fibroblasts were grown to complete confluence or sparse (25% confluence), were transfected with GCS-HA and subsequently treated with nocodazole (33 µM) for 3 hours and then fixed and stained. Intra-Golgi localization of GCS was quantified by line scan analysis. **(F)** GRASP55 KO fibroblasts were grown to complete confluence or sparse (25% confluence) and SL production monitored by [^{3}H] - sphingosine pulse-chase assay. Total GSL levels was quantified and represented as fold changes respect to lowest confluence (25%). **(G)** Fibroblasts (WT and GRASP55 KO) were grown to confluence in 6 well plates and then maintained for 7 days in the presence or absence of PDMP (2 µM) to monitor foci formation. The cells were stained with crystal violet (0.25%) and the number colonies per well were counted and represented. Values are mean ± SD. Data representative of 2 independent experiments. Values are Mean ± SD. n>30 *p <0.05, **p <0.01, ***p <0.001 (Student's t test).